Journal of Inflammation Research

Dovepress
open access to scientific and medical research

Open Access Full Text Article

ORIGINAL RESEARCH

Hypermethylation Effects of Yiqihuoxue Decoction in Diabetic Atherosclerosis Using Genome-Wide DNA Methylation Analyses

Qing-Bing Zhou[1]
Yao Chen[1]
Yan Zhang[1]
Dan-Dan Li[1]
Hong-Qin Wang[1]
Zi-Jun Jia[1]
Yu Jin[2]
Feng-Qin Xu[1]
Ying Zhang[1]

[1]Institute of Geriatric Medicine, Xiyuan Hospital, China Academy of Chinese Medical Sciences, Beijing, 100091, People's Republic of China; [2]The First Affiliated Hospital of Shenzhen University, Shenzhen Second People's Hospital, Shenzhen, 518035, People's Republic of China

Correspondence: Feng-Qin Xu; Ying Zhang
Institute of Geriatric Medicine, Xiyuan Hospital, Xiyuan Playground No. 1, Haidian District, Beijing, 100091, People's Republic of China
Tel/Fax +86 10-62835003
Email dr.xufengqin@outlook.com

Ying Zhang
Email doctoronline@126.com

Purpose: To investigate if a traditional Chinese medicine formulation, called "Yiqihuoxue" (YQHX), could improve diabetic atherosclerosis (DA) and explore potential mechanisms based on DNA methylation.

Methods: Apolipoprotein E-knockout mice were administered streptozotocin (50 mg/d, i.p.) for 5 days and fed a high-fat diet for 16 weeks. Mice were divided randomly into DA model, rosiglitazone, as well as low-, medium-, and high-dose YQHX groups. Ten healthy C57BL/6J mice were the control group. Serum levels of fasting insulin, blood glucose, homeostasis model-insulin resistance index (HOMA-IR), serum lipids, and inflammatory factors were analyzed after the final treatment. Aorta tissues were collected for staining (hematoxylin and eosin, and Oil red O). Genomic DNA was extracted for methyl-capture sequencing (MC-seq). Kyoto Encyclopedia of Genes and Genomes (KEGG) and Search Tool for the Retrieval of Interacting Genes/Proteins (STRING) databases were used to analyze differentially methylated genes. Pyrosequencing was used to verify MC-seq data.

Results: Low-dose and high-dose YQHX could reduce the HOMA-IR ($P < 0.05$). Low-dose YQHX reduced expression of total cholesterol (TC), low-density lipoprotein-cholesterol (LDL-C), TNF-α, andI L-6 in serum compared with that in the model group ($P < 0.05$). Medium-dose YQHX decoction inhibited the expression level of TNF-α ($P < 0.05$). High-dose YQHX decreased the expression level of IL-6 ($P < 0.05$). Staining also showed the anti-atherosclerosis effects of YQHX ($P < 0.05$). MC-seq revealed many abnormally hypermethylated and hypomethylated genes in DA mice compared with those in the control group. KEGG database analysis showed that the hypermethylated genes induced by YQHX treatment were related to pathways in cancer, Hippo signaling, and mitogen activated protein kinase. The network analysis suggested that the hypermethylated genes epidermal growth factor receptor (*Egfr*) and phosphoinositide-3-kinase regulatory subunit 1(*Pik3r1*) induced by YQHX treatment had important roles in DA. Pyrosequencing revealed that YQHX treatment increased methylation of *AKT1, Nr1h3* and *Fabp4* significantly ($P < 0.05$).

Conclusion: YQHX decoction had positive treatment effects against DA, because it could regulate aberrant hypomethylation of DNA.

Keywords: diabetic atherosclerosis, YQHX decoction, DNA methylation, hypermethylation

Introduction

The prevalence of diabetes mellitus (DM) is increasing worldwide, and DM constitutes a serious public-health problem. Atherosclerosis is a chronic inflammatory disease. It is an important pathologic basis for the development of various cardiovascular and cerebrovascular diseases. Patients with DM carry a higher risk of

Received: 25 August 2021
Accepted: 3 December 2021
Published: 8 January 2022

developing atherosclerosis, and diabetic atherosclerosis (DA) is a major cause of death in DM patients.[1] The mechanisms linking DM and atherosclerosis center mainly around endothelial-cell dysfunction, the inflammatory response, changes in mitochondrial oxidative stress, and DNA methylation; aberrant methylation of DNA is thought to be a potential and novel therapeutic target for patients with DA.[2]

DNA methylation (ie, an addition of a methyl group to cytosine mediated by DNA methyltransferases) is a vital modification of the genome in cells.[3] DNA methylation can regulate gene expression and plays an important part in the development of DM, atherosclerosis, and DA. Studies have indicated that changes in DNA methylation may drive the development of type-2 diabetes mellitus (T2DM).[4] Genome-wide analysis of DNA methylation has revealed T2DM patients have many aberrantly methylated genes related to insulin resistance, lipid transport, adipogenesis, cell proliferation, and cell differentiation. For example, the insulin resistance-related genes insulin receptor substrate 1(*IRS1)*, JAZF zinc finger 1(*JAZF1)*, membrane-associated ring finger (C3HC4) 1(*MARCH1*) and transcription factor 7 like 2(*TCF7L2*) are hypomethylated in T2DM patients.[5] Functional studies have revealed the methylation status of *glutathione S-transferase theta 1 (GSTT1*), glutathione peroxidase 7 (*GPX7*), and sorting nexin 19 (*SNX19)* is correlated with messenger (m)RNA expression and that these genes could affect the proliferation and apoptosis of pancreatic-islet β-cells directly.[6] Reports have also suggested that aberrant DNA methylation is probably the core mechanism in atherosclerosis development.[7–9]Aberrant methylation of DNA could cause inflammation and accelerate atherosclerosis. Kruppel-like factors are zinc-finger proteins and important anti-inflammatory factors.[10] Aberrant hypermethylation and low expression of Kruppel-like factor-4 has been observed in human aortic endothelial cells, which can lead to inflammation in atherosclerotic areas.[8] Moreover, increasing evidence suggests that DNA methylation has a substantial role in DA development through "metabolic memory" (ie, the complications of T2DM induced by early hyperglycemia can persist even though the blood glucose level of DM patients is controlled to a normal level).[11] Studies have shown that DNA methylation at key 5′—C—phosphate—G—3′ (CpG) sites is associated with the onset of complications in patients with T2DM continues for 10 years.[11] Considering the importance of DNA methylation in the development of complications in T2DM, DNA methylation is thought to be a therapeutic target for DA.

Traditional Chinese medicine (TCM) has been employed in China for more than 3000 years. TCM theory dictates that "Qi and Yin deficiency" and "blood stasis" are the main causes of DA.[12] We hypothesized that a decoction called "Yiqihuoxue" (YQHX) could promote blood circulation and tonify qi and yin and, therefore, be employed for DA treatment.

We investigated the treatment effect of YQHX and elucidated its mechanism of action from the perspective of DNA methylation. Analysis of genome-wide methylation was undertaken to observe the effects of YQHX on DNA methylation in a mouse model of DA, and differentially methylated genes in different groups were identified. Next, the differentially methylated genes were analyzed using Kyoto Encyclopedia of Genes and Genomes (KEGG; www.genome.jp/kegg/pathway.html/) and Search Tool for the Retrieval of Interacting Genes/Proteins (STRING) 11 databases (https://string-db.org/). Finally, three CpG sites from the genome-wide methylation data were chosen for validation by pyrosequencing.

Materials and Methods

Main Herbs and Reagents

YQHX is composed of *Ligusticum wallichii* (LW), red peony root (RPR), and *Panax quinquefolius* saponins (PQS), all of which were supplied by Xiyuan Hospital (Beijing, China). These three components were mixed at a 40:20:1 ratio and made into a liquid extract by the Pharmacy Department of Xiyuan Hospital. Each milliliter of the liquid extract contained LW (0.96 g), RPR (0.48 g) and PQS (0.024 g). Rosiglitazone (Shenjitang, Guizhou, China) was dissolved in physiologic (0.9%) saline to make a stock solution of 0.5 mg/mL.

Animals and Experimental Design

The animal experiment program was approved by the Ethical Committees of Xiyuan Hospital, affiliated to China Academy of Chinese Medical Sciences. Animal treatments conformed to the "Advice on the treatments of experimental animals" issued by the Ministry of Science and Technology of China (Beijing, China) and the International Council for Laboratory Animal Science (ICLAS). Fifty male apolipoprotein E (ApoE)-knockout mice (6 weeks) were purchased from Beijing Tonglihua (production license number: SCXK 2016–0011). ApoE-knockout mice were injected with

streptozotocin (50 mg/d, i.p.; Sigma–Aldrich, Saint Louis, MO, USA) for 5 days and, after 1 week of adaptive feeding, fed high-fat chow with basic feed 78.85%, lard 21%, cholesterol 0.15% for 16 weeks. Then, mice were randomly divided into five groups of 10: (1) DA model; (2) rosiglitazone (fed with rosiglitazone (6.5 g/kg·d) for 6 weeks); (3) low-dose YQHX (fed with LW (2.4 g/kg·d), RPR (1.2 g/kg·d) and PQS (60 mg/kg·d) for 6 weeks; (4) medium-dose YQHX (fed with LW (4.8 g/kg·d), RPR (2.4 g/kg·d) and PQS (120 mg/kg·d) for 6 weeks; (5) high-dose YQHX (fed with LW (9.6 g/kg·d), RPR (4.8 g/kg·d) and PQS (240 mg/kg·d) for 6 weeks. Ten healthy C57BL/6J mice were used as a control group.

Measurement of Insulin, Blood Glucose, Homeostasis Model-Insulin Resistance Index (HOMA-IR), Serum Lipids, and Inflammatory Factors

Fasting insulin levels were analyzed by an Iodine [^{125}I] Insulin Radioimmunoassay Kit (Beifang Biotechnology, Beijing, China) according to manufacturers' instructions. Glucose levels in blood were tested in a blood sample obtained from the tail vein of mice every week. The formula "(fasting blood-glucose × fasting insulin)/22.5" was applied to calculate HOMA-IR. Serum was obtained and retained at −80 °C. Then, an automatic biochemical analyzer (Beckman Coulter, Fullerton, CA, USA) was used to measure the levels of total cholesterol (TC), low-density lipoprotein-cholesterol (LDL-C), triglycerides (TG) and high-density lipoprotein-cholesterol (HDL-C) in different groups. Expression of interleukin (IL)-6 and tumor necrosis factor (TNF)-α in different groups was measured by an enzyme-linked immunosorbent assay (BioTek, Winooski, VT, USA) according to manufacturers' protocols.

Staining

Staining (hematoxylin and eosin (H&E) and Oil Red O (ORO) was undertaken to observe lipid accumulation in the aorta, and areas of lipid plaques. After the final treatment, the aorta was collected from each killed mouse. Aorta samples were fixed in 4% paraformaldehyde. Paraffin sections were cut at thicknesses of 5 μm for H&E staining. Microscopic examination was undertaken to assess atherosclerotic changes in the aorta. To observe the plaque area of the whole aortas, ORO staining was applied, as described previously.[13]

High-Throughput Analyses of Methylomes

Methylation status in 30 aorta samples from each group (except the rosiglitazone group) was analyzed by methyl-capture sequencing (MC-seq) using a system from Agilent Technologies (Santa Clara, CA, USA). Briefly, genomic DNA was extracted from 30 aorta samples using the DNeasy® Blood & Tissue kit (Qiagen, Stanford, VA, USA) according to manufacturers' instructions. Qubit™ 2.0 and agarose-gel electrophoresis were used to quantify DNA (Invitrogen, Carlsbad, CA, USA). Genomic DNA (3 μg) was fragmented to a peak size of 100–170 bp. According to the protocol for the MC-seq system, 350 ng of DNA was mixed with blocking mixes, hybridization buffers, and RNase block to capture the methylation region. We applied the EZ DNA Methylation™ kit (Zymo Research, Irvine, CA, USA) to convert the DNA. After bisulfite treatment, the captured DNAs were subjected to amplification by polymerase chain reaction (PCR). Then, the HiSeq™ 2500 platform (Illumina, San Diego, CA, USA) was applied to sequence the bisulfite-converted DNA. The raw data generated from sequencing was checked and had to meet the quality-control criteria set by Illumina. Differentially methylated sites were identified, and the corresponding genes were analyzed using the KEGG database (a key bioinformatics tool for finding signaling pathways).[14]

Protein–Protein Interaction (PPI) Networks

Differentially methylated genes were obtained and evaluated using the STRING 11 database. Network construction was carried out by Cytoscape 3.5.0 (https://cytoscape.org/). A high confidence score with a correlation degree ≥0.700 as the cutoff value was set to obtain a PPI network.

Methylation Validation by Pyrosequencing

Three differentially methylated sites in different groups according to MC-seq were chosen for pyrosequencing. Briefly, the primers used for the chosen genes were designed by PyroMark® Assay Design 2.0 (Qiagen) and the primers are listed in Table S1. Next, bisulfite-treated DNA was subjected to PCR with the following cycling parameters: 98 °C for 10 s, 55 °C for 30 s, and 72 °C for 30 s for 35 cycles. Then, the PCR products were sent for sequencing using the PyroMark Q96 system (Qiagen). Finally, Pyro Q-CpG™ was applied to quantify the level of DNA methylation of each CpG site in different groups.

Statistical Analyses

Differences in the levels of insulin, blood glucose, serum lipids, inflammatory factors, and the methylation levels of sites among different groups were assessed by Student's *t*-tests or one-way analysis of variance. $P < 0.05$ was considered significant. The significance of differences in methylation levels in the five groups was evaluated by Bayesian and linear regression analysis. CpG sites with a change of ±0.1 in β-values (delta beta) and $P < 0.05$ in the different groups were considered significant.

Results

Levels of Blood Glucose, Insulin, and the HOMA-IR

Compared with mice in the control group, the blood glucose level and IR of mice in the model group increased

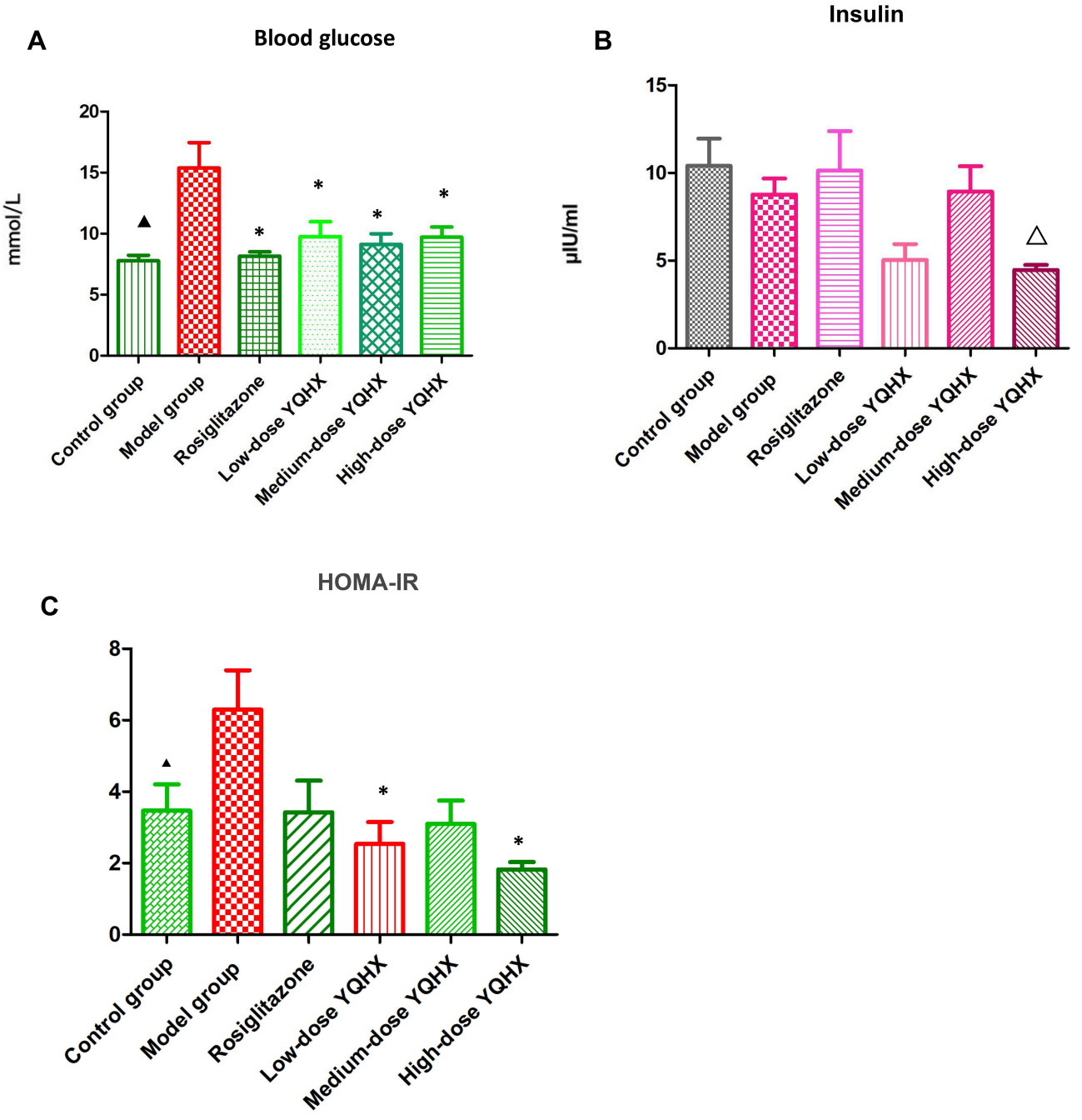

Figure 1 Effects of YQHX on levels of blood glucose, insulin, and HOMA-IR. (**A**) Blood glucose; (**B**) insulin; (**C**) HOMA-IR. Error bars indicate mean ± SEM (n = 6). ▲$P < 0.05$ compared with the model group; *$P<0.05$ compared with the model group; Δ$P<0.05$ compared with the control group.

significantly ($P < 0.05$) (Figure 1). Blood glucose levels in all treatment groups were significantly lower than those in the model group ($P < 0.05$ for all) (Figure 1A). Insulin levels among all groups did not change significantly ($P > 0.05$) (Figure 1B). The IR in high-dose and low-dose YQHX groups was reduced significantly ($P < 0.05$), but the decrease in the medium-dose YQHX group and rosiglitazone group was not significant ($P > 0.05$) (Figure 1C).

Serum Lipid Profiles

Twenty-two weeks after administration, the higher serum levels of TC and LDL-C, and lower levels of HDL-C were observed in the model group when compared with those in the control group ($P < 0.05$) (Figure 2A, B and D). Compared with those in the model group, mice in the low-dose YQHX group had reduced levels of LDL-C and TC ($P < 0.05$), but the difference in the expressions of TC and

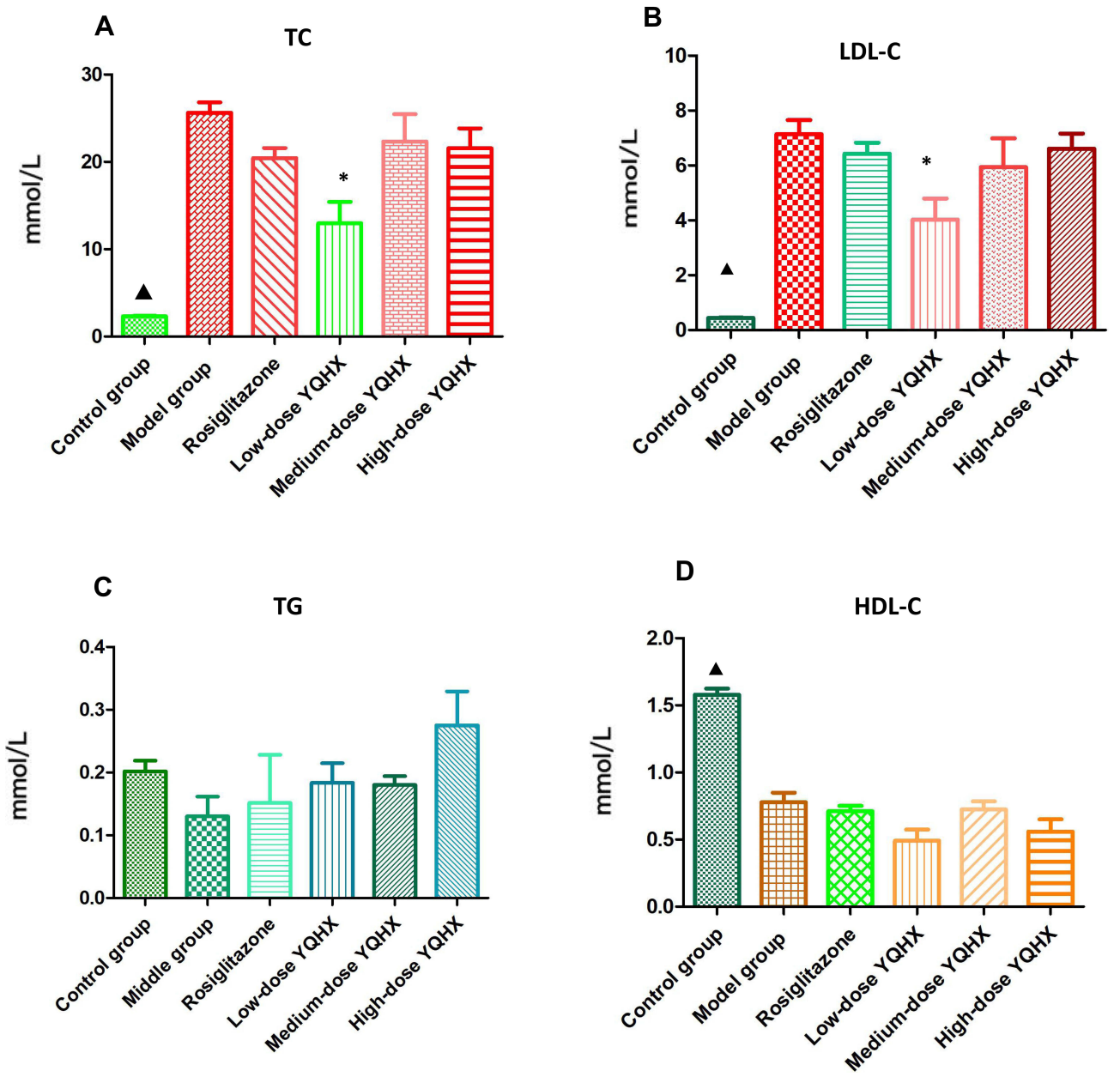

Figure 2 Effects of YQHX on levels of serum lipids. (**A**) TC; (**B**) TG; (**C**) LDL-C; (**D**) HDL-C. Error bars indicate mean ± SEM (n = 6). ▲$P < 0.05$ compared with the model group; *$P < 0.05$ compared with the model group.

LDL-C in the rosiglitazone group, medium-dose YQHX group, and high-dose YQHX group was not significant ($P > 0.05$) (Figure 2A and B). Significant differences for TG and HDL among the treatment groups were not observed (Figure 2C and D).

Expression of TNF-α and IL-6 in Serum

Compared with that in the control group, expression of TNF-α and IL-6 in the model group increased significantly ($P < 0.01$); rosiglitazone treatment reduced TNF-α expression significantly ($P < 0.01$), but had no effect on IL-6 expression ($P > 0.05$). Expression of TNF-α and IL-6 was significantly lower in the low-dose YQHX group than that in the model group ($P < 0.05$); medium-dose YQHX reduced TNF-α expression ($P < 0.05$), but had no effect on IL-6 expression; high-dose YQHX could decrease IL-6 expression, but had no effect on TNF-α expression ($P > 0.05$) (Figure 3).

Morphology

The morphology of the aorta wall in mice of each group is displayed in Figure 4. ORO staining showed the whole aortic area of mice in the model group have greater red-stained lipid accumulation compared with that in the control group. Compared with that in the model group, lipid content was less abundant in all treatment groups ($P < 0.05$) (Figure 4A and B). H&E staining revealed the area of atherosclerotic plaques increased in the model group compared with that in the control group, and that treatment with YQHX (all doses) and rosiglitazone could reduce the area of atherosclerotic plaques ($P < 0.05$) (Figure 4C and D).

Many Abnormally Methylated Genes in the Model Group

Compared with the sites in the control group, 36,092 sites were significantly hypomethylated and 22,677 sites were aberrantly hypermethylated in the model group, which corresponded to 8013 hypomethylated and 6014 hypermethylated genes, respectively (Figure 5A, Table S2). Figure 5B shows the distribution of differently methylated sites in the positions of genes. Analyses of the top-30 signaling pathways revealed that the aberrant hypomethylated or hypermethylated genes play an important role in many DA-related pathways and functions, including Wnt signaling pathway, Hippo signaling pathway, and T2DM (Figure 5C).

YQHX Treatment Altered DNA Methylation in Mice with DA

Compared with the sites in the model group, there were 153,324 hypermethylated sites and 42,732 hypomethylated sites in the low-dose YQHX group, which corresponded to 13,250 (67.26%) hypermethylated genes and 6449 (32.74%) hypomethylated genes, respectively (Figure 6A, Table S3). After treatment with medium-dose YQHX, 209,814 sites were changed significantly, which corresponded to 20,909 genes. Among these 20,909 genes,

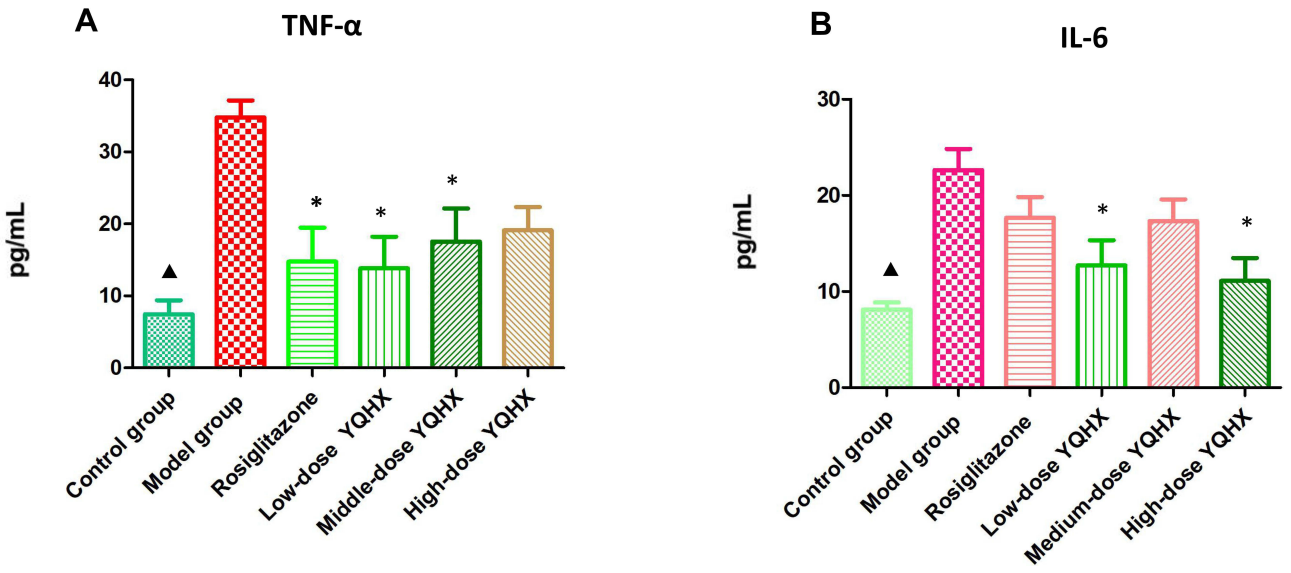

Figure 3 Effects of YQHX on expression of tumor necrosis factor (TNF)-α and interleukin (IL)-6. (**A**) TNF-α; (**B**) IL-6. Error bars indicate mean ± SEM (n = 6). ▲$P < 0.05$ compared with the model group; *$P<0.05$ compared with the model group.

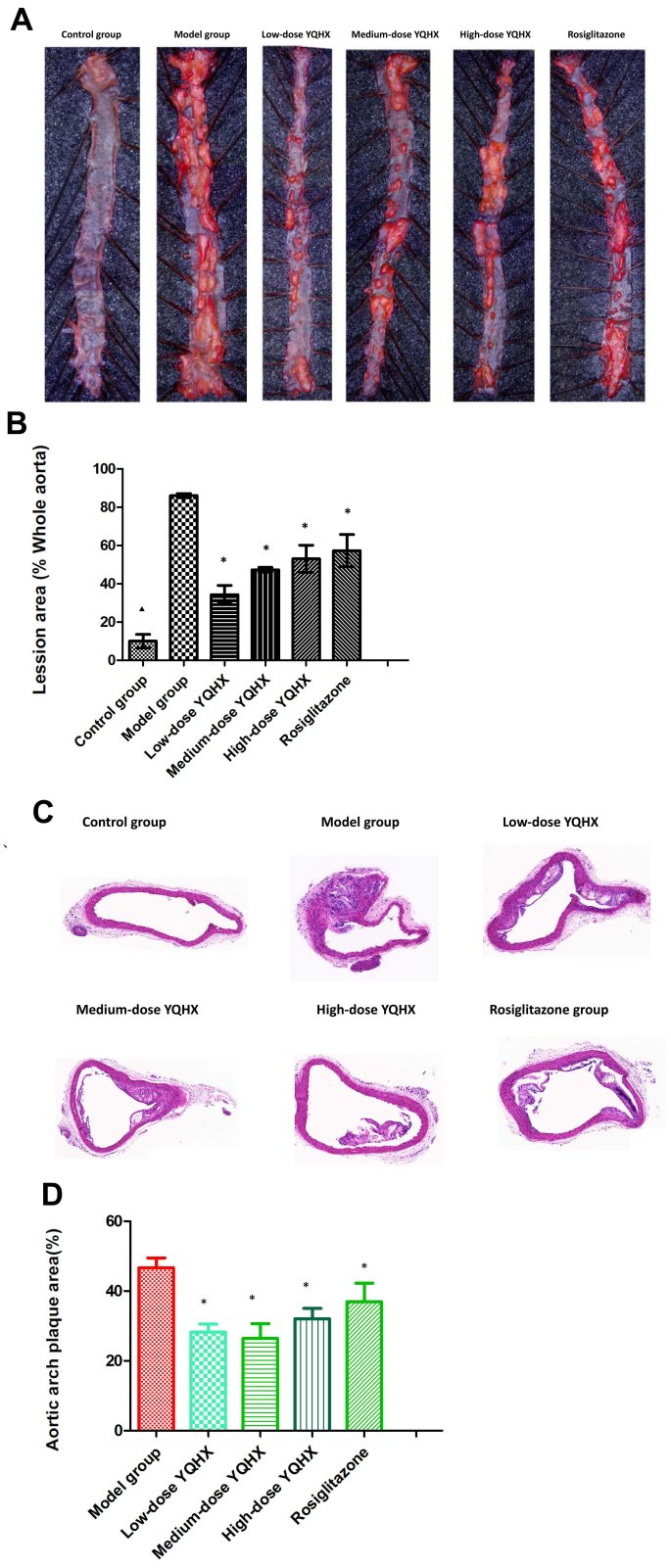

Figure 4 Pathologic staining of atherosclerotic lesions. (**A**) Whole aortic area by Oil red O staining; (**B**) percentage of lipid accumulation; (**C**) representative photographs of aortic lesions from H&E staining (magnification × 200); (**D**)percentage of plaque area. The error bars indicate mean ± SEM (n=3). ▲ $P<0.05$, compared with the model group; * $P<0.05$, compared with the model group.

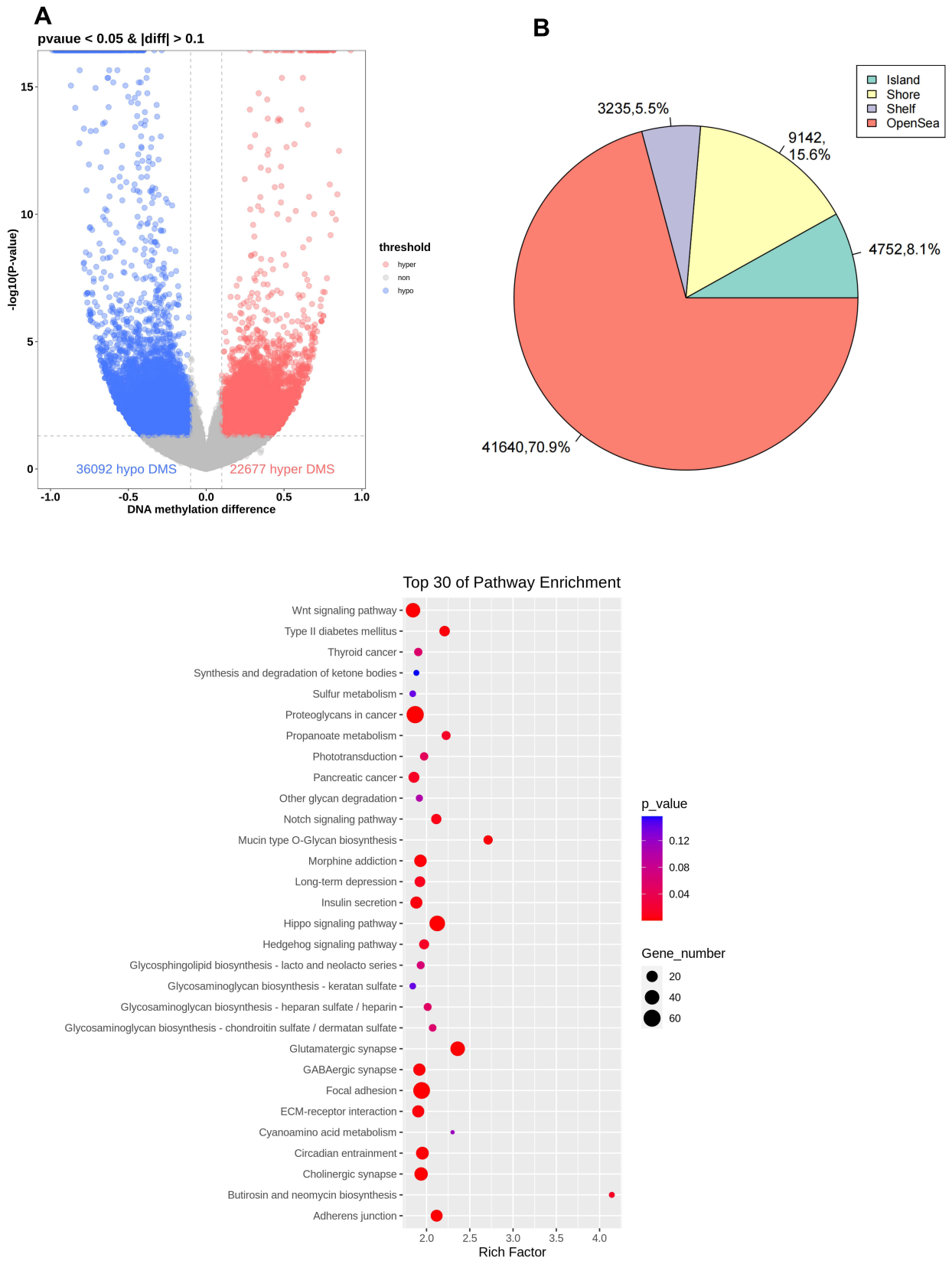

Figure 5 Differential methylation of six aorta samples from the model group versus those from the control group. (**A**) Volcano plot of methylation sites. Hypomethylated sites are blue and hypermethylated sites are red. Dotted lines delineate ±0.1 methylation differences and represent a threshold of 0.05 for *P*. (**B**) Distribution of differently methylated sites in the positions of genes in the model group compared with that in the control group. (**C**) Top-30 KEGG terms for aberrantly methylated genes in the model group.

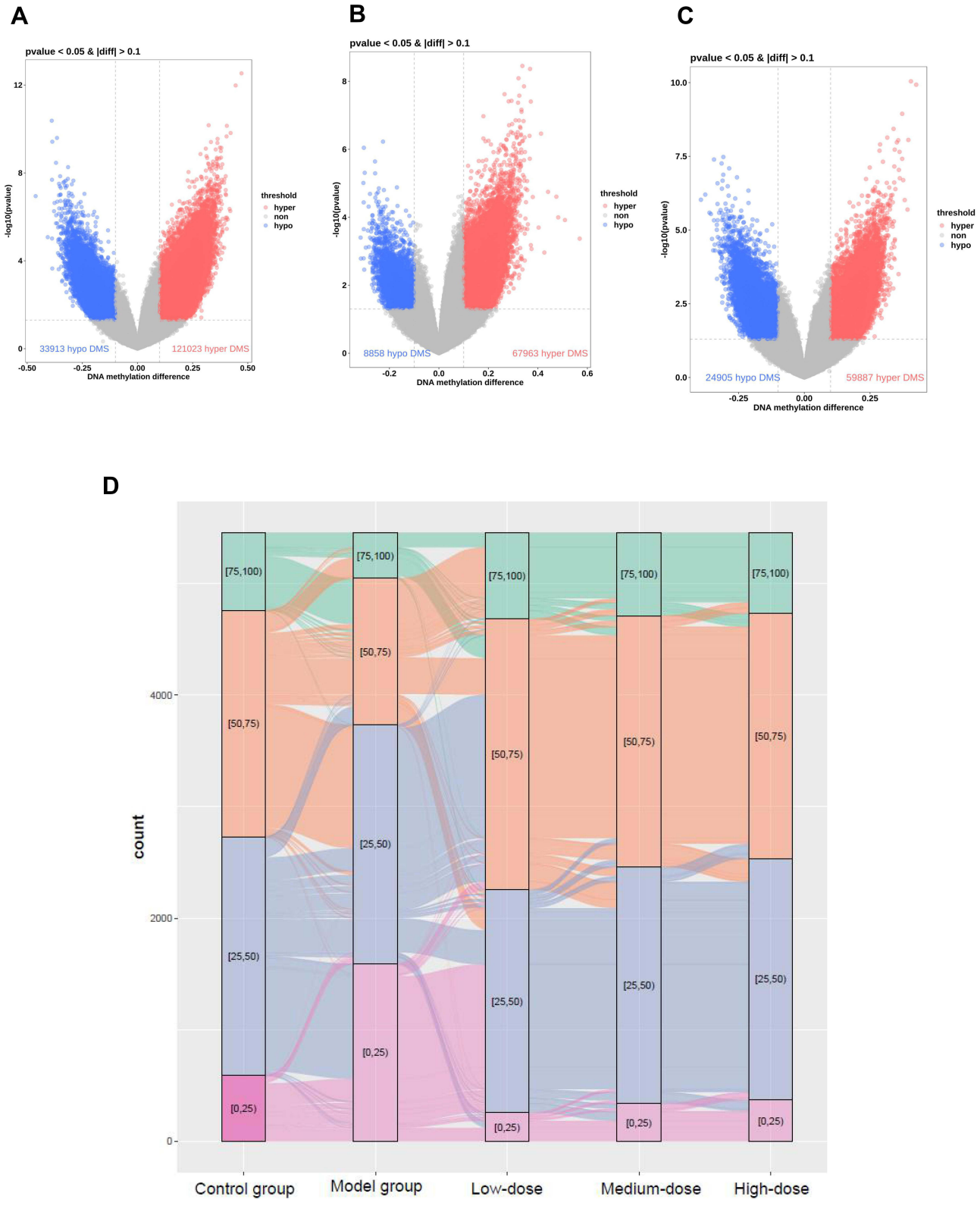

Figure 6 General information about YQHX effects on DNA methylation in mice with DA. Volcano plots of methylation for significant CpG sites. Hypomethylated probes are blue and hypermethylated probes are red. Dotted lines delimit ±0.1 methylation differences between YQHX-treated groups vs control group, and represent a *P*-value threshold of 0.05. Compared with those in the model group, differentially methylated sites are shown in the low- (**A**), medium- (**B**) and high-dose YQHX (**C**) groups, respectively. (**D**) Alluvial diagram showing the distribution of differentially methylated sites among different groups.

Table 1 KEGG Analysis of Identified Hypermethylated Genes from Low-Dose YQHX Group Comparing with Those in Model Group

Pathway	Gene Symbol	P value	Q Value
Pathways in cancer	Ccnd1, Pparg, Nfkb1, Arnt2, Skp2, Crkl, Stat1, Tgfbr1, Stk4, Apc, Rac1, Fzd10, Prkca, Egf	6.93E-07	0.00018
Hippo signaling pathway	Ccnd1, Lats2, Mob1b, Tgfbr1, Apc, Csnk1d, Pard6a, Ctnnb1, Fzd10, Tgfb1, Bmpr2, Tcf7l1	7.46E-07	1.00E-04
Focal adhesion	Ccnd1, Crkl, Mylpf, Itga1, Pdpk1, Rac1, Ctnnb1, Col27a1, Prkca, Egf, Itga3, Col1a2, Mapk10	1.84E-06	0.00012
PI3K-Akt signaling pathway	ICcnd1, Irs1, Nfkb1, Tlr2, Itga1, Pdpk1, Gng2, Rac1, Col27a1, Prkca, Egf, Itga3, Creb3l4	6.48E-05	0.00347
Calcium signaling pathway	Cacna1b, Htr5a, Tacr1, Ryr3, Adcy9, Prkca, Chp1, Grin2a, Ppp3r1, Atp2a2	0.0038	0.027
MAPK signaling pathway	Nfkb1, Crkl, Rps6ka6, Cacna1b, Tgfbr1, Stk4, Rac1, Map3k8	0.0005	0.0089
Insulin signaling pathway	Irs1, Crkl, Hk3, Gck, Pdpk1, Irs2, Ptpn1, Pde3a, Mapk10, Prkag2	0.0004	0.009
Wnt signaling pathway	Ccnd1, Apc, Rac1, Wif1, Ctnnb1, Fzd10, Prkca, Chp1, Ppp3r1, Camk2b, Mapk10	0.0079	0.046

Abbreviation: KEGG, Kyoto Encyclopedia of Genes and Genomes.

14,833 (70.94%) genes were hypermethylated and 6076 (29.06%) genes were demethylated (Figure 6B, Table S4). There were 110,091 differentially methylated sites in the high-dose YQHX group compared with those in the model group, which corresponded to 10,436 (60.94%) hypermethylated genes and 6687 (39.06%) hypomethylated genes, respectively (Figure 6C, Table S5).

An alluvial diagram exhibited the distribution of differentially methylated sites among different groups (Figure 6D). Analyses of signaling pathways using the KEGG database exhibited that the hypermethylated genes induced by YQHX treatment were closed to cancer-associated pathways, Hippo, mitogen-activated protein kinase (MAPK) and phosphoinositide 3-kinase/protein kinase B (PI3K-Akt). The parts of the pathways and related genes are listed in Tables 1, 2, and S6.

PPI Network Analyses of Differentially Hypermethylated Genes Induced by YQHX

Among the 13,250 hypermethylated genes in the low-dose group when compared with those in the model group, we chose the top-500 hypermethylated genes according to absolute deviation for the network analysis. In the PPI network, some nodes including epidermal growth factor receptor(*Egfr*), phosphoinositide-3-kinase regulatory subunit 1(*Pik3r1*) and Paxillin (*Pxn*) had higher degrees (Figure 7). We also imported hypermethylated genes induced by medium-dose YQHX and high-dose YQHX to the STRING database for network analyses (Figures S1 and S2, respectively).

Table 2 KEGG Analysis of Identified Hypermethylated Genes from Medium-Dose YQHX Group Comparing with Those in Model Group

Pathway	Gene Symbol	P value	Q Value
Pathways in cancer	Mapk1, Ncoa4, Smo, Pik3r1, Fgf5, Shh, Itga2b, Fos, Wnt11, Pik3ca	2.49E-05	0.0016
Hippo signaling pathway	Snai2, Ppp2r1b, Dlg2, Wnt11, Ccnd3, Ywhah, Wnt6, Trp73, Tead4	1.67E-05	0.0014
Focal adhesion	Mapk1, Pak7, Col2a1, Pik3r1, Itga2b, Ccnd3, Pik3ca, Vwf, Myl9	6.08E-07	0.0001
Axon guidance	Ephb2, Mapk1, Pak7, Unc5b, Gnai1, Dpysl5, Nck2, Plxnc1, Limk1	7.08E-05	0.003
PI3K-Akt signaling pathway	Mapk1, Ppp2r1b, Col2a1, Pik3r1, Fgf5, Angpt4, Itga2b, Ghr, Ccnd3	0.00082	0.0405
HIF-1 signaling pathway	Mapk1, Pik3r1, Angpt4, Hk1, Mknk1, Pik3ca, Insr, Ldha, Eif4ebp1, Angpt2	0.0015	0.017
MAPK signaling pathway	Fgf10, Relb, Sos1, Ppp3ca, Cdc42, Mapk9, Prkaca, Fgf23, Tgfbr1, Tgfb2	0.0003	0.0612
Metabolic pathways	Dld, Ugdh, Polr1e, Hgsnat, Tat, Qdpr, Ndufa4l2, Nos1, Paics, Alpl	0.003	0.024
Estrogen signaling pathway	Mapk1, Gnai1, Pik3r1, Fos, Pik3ca, Creb5, Atf2, Adcy6, Kcnj9, Gabbr2	0.0002	0.006

Abbreviation: KEGG, Kyoto Encyclopedia of Genes and Genomes.

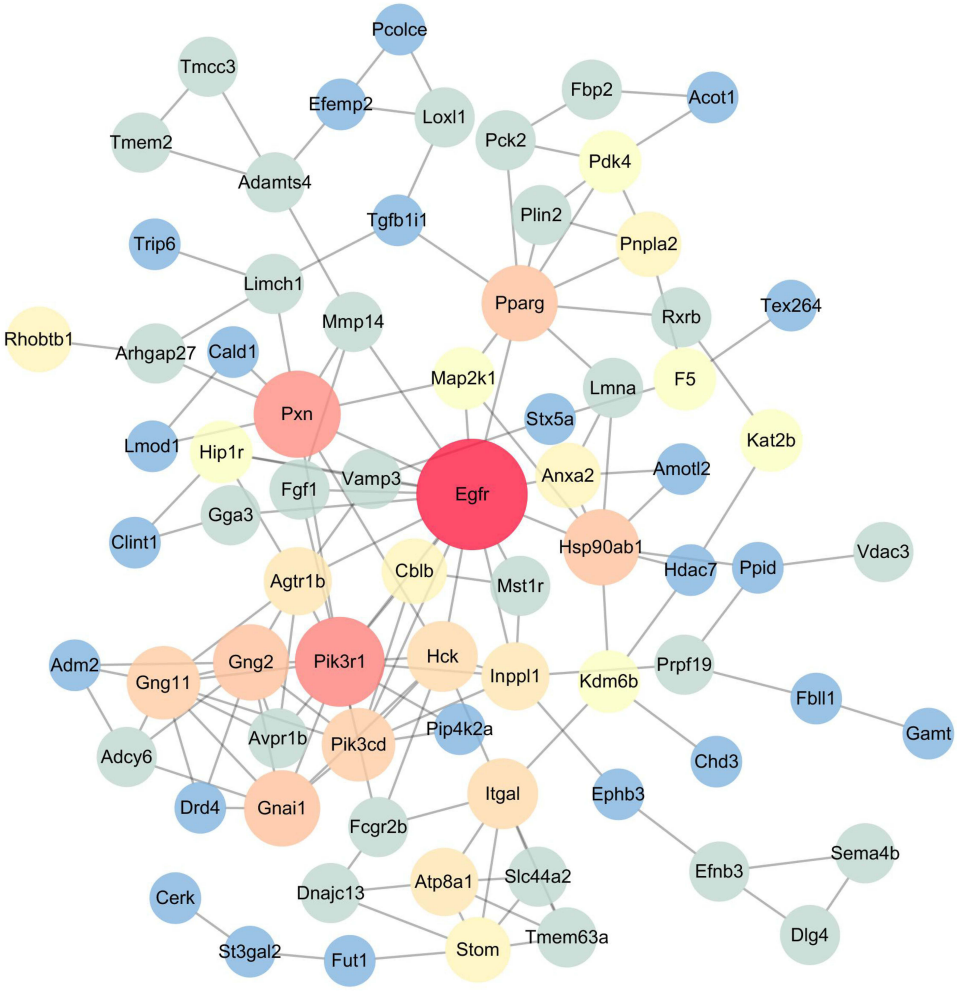

Figure 7 Low-dose YQHX–DA PPI network analysis. Compared with those in the model group, the top-500 hypermethylated genes in the low-dose YQHX group were chosen for PPI network analysis using the STRING database. The size and color of the node represent the value of degree. The deeper the color, the higher the degree. The red nodes (*Egfr, Pik3r1, Pxn*) have higher degrees. The node size of genes is proportional to the number of degrees.

Hypermethylation Effects of YQHX According to Pyrosequencing

To further demonstrate the hypermethylation effects of YQHX, pyrosequencing was applied to check the methylation status of three CpG sites corresponding to AKT serine/threonine kinase 1(*AKT1)*, nuclear receptor subfamily 1 group H member 3(*Nr1h3*) and fatty acid binding protein 4 (*Fabp4)*. These three sites were hypomethylated significantly in the control group ($P < 0.05$ for both) compared with those in the model group (Figure 8). After treatment with YQHX, the methylation of AKT1, Nr1h3, and Fabp4 in all treatment groups increased significantly, which was consistent with MC-seq data.

Discussion

We addressed, for the first time, the effects of YQHX treatment on mice suffering from DA. We demonstrated that this treatment could improve aberrant hypomethylation in mice with DA. Our study indicated that YQHX could be an innovative hypermethylation agent for DA treatment in the future.

DA is the main macrovascular complication of DM.[15] Emerging evidence suggests that finding efficacious therapeutic drugs from TCM formulations could be an important strategy in DA cure.[16] In the present study, YQHX showed a remarkable effect against DA in vivo. First, ApoE-knockout mice were injected with streptozotocin and fed a high-fat diet: the blood glucose level, IR, TC level, and LDL-C level of mice in the model group increased significantly. ORO staining displayed the accumulation of red-stained lipids when compared with that in the control group, which demonstrated that the DA model had been created. The blood glucose level in all treatment groups decreased when compared with that in

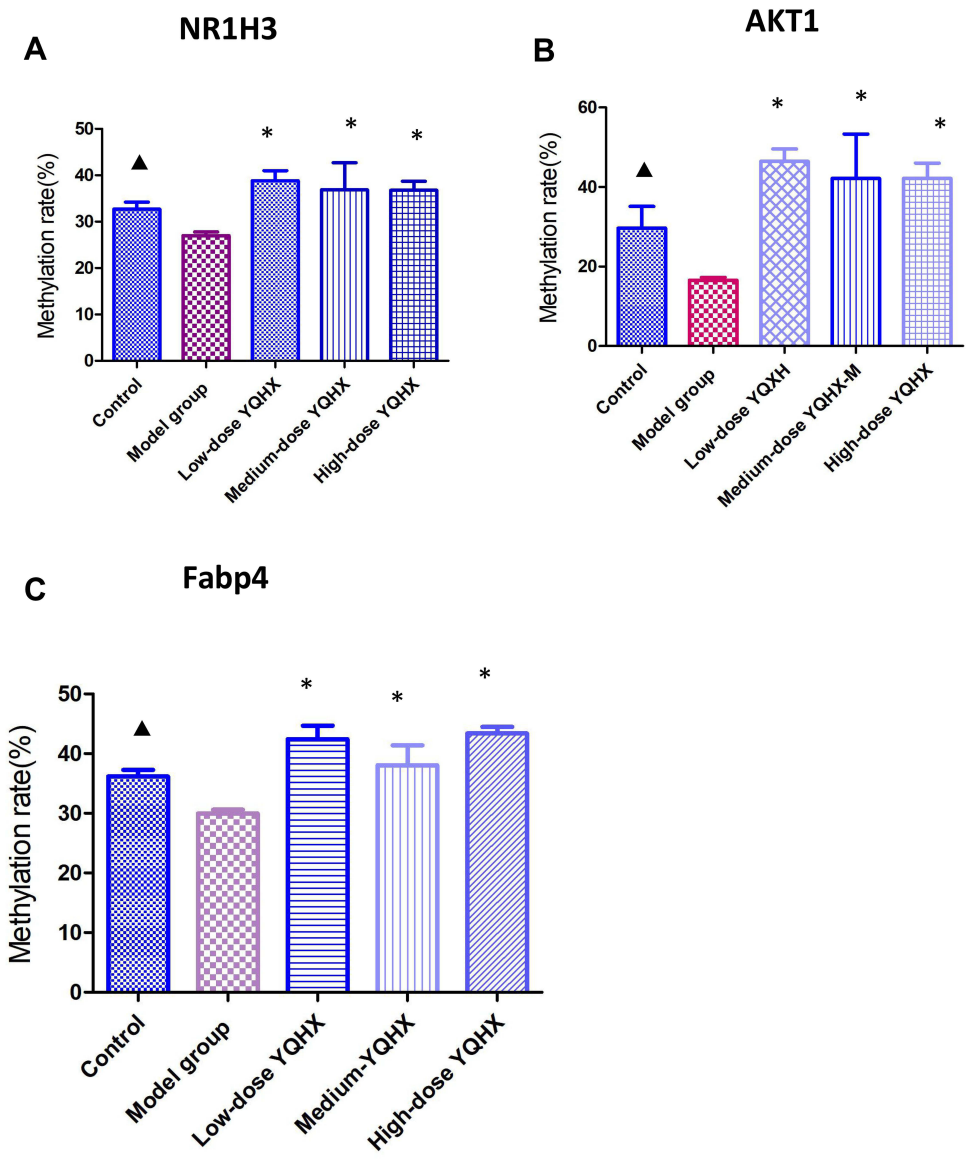

Figure 8 Effects of YQHX on methylation of NR1H3, AKT1, and Fabp4 according to pyrosequencing. (**A**) NR1H3; (**B**) AKT1; (**C**) Fabp4. Error bars indicate mean ± SEM (n = 6). ▲$P < 0.05$ compared with the model group; *$P < 0.05$, compared with the model group.

the model group. None of the YQHX doses had an effect on the insulin level, but treatment with low-dose and high-dose YQHX could reduce the IR. Moreover, low-dose YQHX could reduce the serum level of TC and LDL-C when compared with those in the model group.

Several studies have highlighted the importance of inflammation in diabetic vascular disease, which leads to accelerated dysfunction of inflammatory cells and vascular cells.[17,18] In the present study, medium-dose and high-dose YQHX could lower expression of only TNF-α or IL-6, respectively. However, low-dose YQHX not only reduced TNF-α expression, it also reduced expression of IL-6, which indicated that low-dose YQHX showed the best anti-inflammatory effect. Staining (H&E and, ORO) also revealed the anti-atherosclerosis effects of YQHX for DA treatment in mice. Taken together, our data demonstrated that YQHX provided a protective effect against DA.

Numerous studies have reported that abnormal methylation of DNA has critical roles in DA development.[19,20] For example, aberrantly hypomethylated genes such as fibroblast growth factor 2(*FGF2*), SMAD family member 3(*SMAD3*), and cyclin dependent kinase inhibitor 1A (*CDKN1A*) were identified in DM patients, and these hypomethylated genes were closely related to pathways in cancer, the MAPK signaling pathway, focal adhesion, and regulation of the actin cytoskeleton.[21] Consistent with

those reports, we also found that many abnormally hypomethylated and hypermethylated genes were present in DA mice compared with those in the control group. Analyses of enriched signaling pathways using the KEGG database revealed that these abnormally methylated genes participated in many DA-related pathways and functions, such as focal adhesion, the Wnt signaling pathway, Hippo signaling pathway, and T2DM, which further demonstrated the importance of DNA methylation in DA. To normalize the aberrant DNA methylation in DA, drugs targeting hypomethylation or hypermethylation are needed. Interestingly, genome-wide analyses of methylation suggested that YQHX treatment mainly induced DNA hypermethylation. The number of hypermethylated genes induced by YQHX treatment was 13,250 (67.26%), 4833 (70.94%), and 10,436 (60.94%) in low-, medium-, and high-dose YQHX groups, respectively, which indicated that YQHX may be a novel hypermethylation agent. Analyses using the KEGG database showed the hypermethylated genes induced by YQHX treatment were related to pathways in cancer, the Hippo signaling pathway, and MAPK signaling pathway. Network analyses also revealed that hypermethylated genes, including *Egfr, Pik3r1*, and *Pxn*, induced by YQHX treatment had important roles in DA. For example, the cell-surface receptor EGFR can regulate the proliferation, migration, and survival of endothelial cells and vascular smooth muscle cells. EGFR promotes endothelial dysfunction, cardiac remodeling, fibrosis, and neointimal hyperplasia.[22–24] Emerging work suggests that blockade of EGFR expression can inhibit the formation of foam cells and cardiovascular inflammation in atherosclerosis. *Pik3r1* plays an important part in the metabolic actions of insulin, and has been associated with insulin resistance.[25] Considering the importance of DNA methylation in DA, these results showed that targeting hypomethylation may be the main mechanism of action of YQHX.

Pyrosequencing was applied to further determine the hypermethylation effects of YQHX. We demonstrated that methylation of three CpG sites corresponding to the genes of AKT1, Nr1h3, and Fabp4 increased after YQHX treatment. AKT1 methylation increased after YQHX treatment. The AKT1 gene encodes one of the three members of the human AKT serine-threonine protein kinase, which is essential for the migration and proliferation of vascular smooth muscle cells.[26,27] Studies have shown that downregulation of AKT1 expression could improve atherosclerosis by inhibiting the migration and growth of vascular smooth muscle cells.[28] *Fabp4* was hypermethylated after YQHX treatment, and has key roles in the uptake, transport, and metabolism of fatty acids. *Fabp4* overexpression is associated with atherosclerosis, obesity, insulin resistance, T2DM, hypertension, ischemic stroke.[29–31] Targeting *Fabp4* may be a good treatment strategy for patients with DA.[32] These observations indicate that YQHX treatment causes hypermethylation of DA-related genes, which may be the main mechanism of action of YQHX in DA treatment. Furthermore, this mechanism is different from that of two inhibitors of DNA methylation, azacitidine and decitabine, which can demethylate aberrantly hypermethylated genes to elicit hypomethylation.[33]

Conclusions

We demonstrated that YQHX had treatment effects on mice with DA. YQHX appeared to regulate aberrant hypomethylation in DA, so YQHX could be an innovative methylation agent. Whether these protective effects translate into better treatment effects for DA patients should be determined in clinical trials.

Funding

This work was supported by China Academy of Chinese Medicine Scientific Foundation (ZZ13-YQ-010), the National Natural Scientific Foundation of China (81774143, 81973679), Sanming Project of Medicine in Shenzhen (SZSM201612049) and the Qihuang Project for Inheritance and Innovation of Traditional Chinese Medicine (02045006).

Disclosure

The authors of this manuscript declare no conflicts of interest.

References

1. Kishore P, Kim SH, Crandall JP. Glycemic control and cardiovascular disease: what's a doctor to do? *Curr Diab Rep*. 2012;12:255–264. doi:10.1007/s11892-012-0268-5
2. La Sala L, Prattichizzo F, Ceriello A. The link between diabetes and atherosclerosis. *Eur J Prev Cardiol*. 2019;26:15–24. doi:10.1177/2047487319878373
3. Suzuki MM, Bird A. DNA methylation landscapes: provocative insights from epigenomics. *Nat Rev Genet*. 2008;9:465–476. doi:10.1038/nrg2341
4. Kim M. DNA methylation: a cause and consequence of type 2 diabetes. *Genomics Inform*. 2019;17(4):e38. doi:10.5808/GI.2019.17.4.e38
5. Nilsson E, Jansson PA, Perfilyev A, et al. Altered DNA methylation and differential expression of genes influencing metabolism and inflammation in adipose tissue from subjects with type 2 diabetes. *Diabetes*. 2014;63(9):2962–2976. doi:10.2337/db13-1459

6. Olsson AH, Volkov P, Bacos K, et al. Genome-wide associations between genetic and epigenetic variation influence mRNA expression and insulin secretion in human pancreatic islets. *PLoS Genet*. 2014;10:e1004735. doi:10.1371/journal.pgen.1004735
7. Scisciola L, Rizzo MR, Marfella R, et al. New insight in molecular mechanisms regulating SIRT6 expression in diabetes: hyperglycaemia effects on SIRT6 DNA methylation. *J Cell Physiol*. 2021;236 (6):4604–4613. doi:10.1002/jcp.30185
8. Jiang YZ, Jiménez JM, Kristy O, et al. Hemodynamic disturbed flow induces differential DNA methylation of endothelial Kruppel-like factor 4 promoter in vitro and in vivo. *Circ Res*. 2014;115 (1):32–43. doi:10.1161/CIRCRESAHA.115.303883
9. Scisciola L, Rizzo MR, Cataldo V, et al. Incretin drugs effect on epigenetic machinery: new potential therapeutic implications in preventing vascular diabetic complications. *FASEB J*. 2020;34 (12):16489–16503. doi:10.1096/fj.202000860RR
10. Yang VW. Mammalian Kruppel-like factors in health and diseases. *Physiol Rev*. 2010;90(4):1337–1381. doi:10.1152/physrev.00058.2009
11. Rosen ED, Kaestner KH, Natarajan R, et al. Epigenetics and epigenomics: implications for diabetes and obesity. *Diabetes*. 2018;67 (10):1923–1931. doi:10.2337/db18-0537
12. Pan L, Li Z, Wang Y, Zhang B, Liu G, Liu J. Network pharmacology and metabolomics study on the intervention of traditional Chinese medicine Huanglian Decoction in rats with type 2 diabetes mellitus. *J Ethnopharmacol*. 2020;258:112842. doi:10.1016/j.jep
13. Yang S, Zhang W, Xuan -L-L, et al. Akebia saponin D inhibits the formation of atherosclerosis in ApoE$^{-/-}$ mice by attenuating oxidative stress-induced apoptosis in endothelial cells. *Atherosclerosis*. 2019;285:23–30. doi:10.1016/j.atherosclerosis.2019.04.202
14. Aoki-Kinoshita KF, Kanehisa M. Gene annotation and pathway mapping in KEGG. *Methods Mol Biol*. 2007;396:71–91.
15. Cecilia C, Wang L. Clinical update: cardiovascular disease in diabetes mellitus. *Circulation*. 2016;133(24):2459–2502. doi:10.1161/CIRCULATIONAHA.116.022194
16. Zhu Q, Kang J, Xu G. Traditional Chinese medicine Shenqi compound to improve lower extremity atherosclerosis of patients with type 2 diabetes by affecting blood glucose fluctuation: study protocol for a randomized controlled multicenter trial. *Medicine*. 2020;99(11): e19501. doi:10.1097/MD.0000000000019501
17. Shanmugam N, Reddy MA, Guha M, Natarajan R. High glucose-induced expression of proinflammatory cytokine and chemokine genes in monocytic cells. *Diabetes*. 2003;52:1256–1264. doi:10.2337/diabetes.52.5.1256
18. Mazzone T, Chait A, Plutzky J. Cardiovascular disease risk in type 2 diabetes mellitus: insights from mechanistic studies. *Lancet*. 2008;371:1800–1809. doi:10.1016/S0140-6736(08)60768-0
19. Jia Z, Jing C, Qian Z, Xinhua X. Novel insights into DNA methylation and its critical implications in diabetic vascular complications. *Bioscience Rep*. 2017;39(2):BSR20160611. doi:10.1042/BSR20160611
20. Pang M, Li Y, Gu W, Sun Z, Wang Z, Li L. Recent advances in epigenetics of macrovascular complications in diabetes mellitus. *Heart Lung Circ*. 2020;30(2):186–196. doi:10.1016/j.hlc.2020.07.015
21. Dayeh T, Volkov P, Salo S, et al. Genome-wide DNA methylation analysis of human pancreatic islets from type 2 diabetic and non-diabetic donors identifies candidate genes that influence insulin secretion. *PLoS Genet*. 2014;10(3):e1004160. doi:10.1371/journal.pgen.1004160
22. Makki N, Thiel KW, Miller FJ Jr. The epidermal growth factor receptor and its ligands in cardiovascular disease. *Int J Mol Sci*. 2013;14:20597–20613. doi:10.3390/ijms141020597
23. Dreux AC, Lamb DJ, Modjtahedi H, Ferns GA. The epidermal growth factor receptors and their family of ligands: their putative role in atherogenesis. *Atherosclerosis*. 2006;186:38–53. doi:10.1016/j.atherosclerosis.2005.06.038
24. Mindur JE, Swirski FK. Growth factors as immunotherapeutic targets in cardiovascular disease. *Arterioscler Thromb Vasc Biol*. 2019;39 (7):1275–1287. doi:10.1161/ATVBAHA.119.311994
25. Karadoğan AH, Arikoglu H, Göktürk F, Işçioğlu F, Ipekçi SH. PIK3R1 gene polymorphisms are associated with type 2 diabetes and related features in the Turkish population. *Adv Clin Exp Med*. 2018;27(7):921–927. doi:10.17219/acem/68985
26. Fernandez-Hernando C, Jozsef L, Jenkins D. Absence of Akt1 reduces vascular smooth muscle cell migration and survival and induces features of plaque vulnerability and cardiac dysfunction during atherosclerosis. *Arterioscler Thromb Vasc Biol*. 2009;29:2033–2040. doi:10.1161/ATVBAHA.109.196394
27. Fernandez-Hernando C, Ackah E, Yu J, et al. Loss of Akt1 leads to severe atherosclerosis and occlusive coronary artery disease. *Cell Metab*. 2007;6:446–457. doi:10.1016/j.cmet.2007.10.007
28. Rotllan N, Wanschel AC, Fernandez-Hernando A, et al. Genetic evidence supports a major role for Akt1 in VSMCs during atherogenesis. *Circ Res*. 2015;116:1744–1752. doi:10.1161/CIRCRESAHA.116.305895
29. Chen L, Zheng S-Y, Yang C-Q, Ma B-M, Jiang D. MiR-155-5p inhibits the proliferation and migration of VSMCs and HUVECs in atherosclerosis by targeting AKT1. *Eur Rev Med Pharmacol Sci*. 2019;23:2223–2233. doi:10.26355/eurrev_201903_17270
30. Furuhashi M, Tuncman G, Gorgun CZ. Treatment of diabetes and atherosclerosis by inhibiting fatty-acid-binding protein aP2. *Nature*. 2007;447(7147):959–965. doi:10.1038/nature05844
31. Chow WS, Tso AW, Xu A, et al. Elevated circulating adipocyte-fatty acid binding protein levels predict incident cardiovascular events in a community-based cohort: a 12-year prospective study. *J Am Heart Assoc*. 2013;2(1):e004176. doi:10.1161/JAHA.112.004176
32. Hotamisligil GS, Johnson RS, Distel RJ, et al. Uncoupling of obesity from insulin resistance through a targeted mutation in aP2, the adipocyte fatty acid binding protein. *Science*. 1996;274 (5291):1377–1379. doi:10.1126/science.274.5291.1377
33. Heuser M, Yun H, Thol F. Epigenetics in myelodysplastic syndromes. *Semin Cancer Biol*. 2018;51:170–179. doi:10.1016/j.semcancer.2017.07.009